Quasi-Static Electromagnetic Dosimetry: From Basic Principles to Examples of Applications

Daniele Andreuccetti
Nicola Zoppetti

Institute for Applied Physics "Nello Carrara"
of the Italian National Research Council (IFAC-CNR), Italy

An overview of quasi-static electromagnetic dosimetry is presented. After an introductive description of quantities and standards and a quick look at experimental and analytical approaches, attention is focused on numerical dosimetry. The process that leads to the calculation of results is analyzed in its basic steps, including the representation of the human body by means of a realistic voxel phantom. The most popular numerical methods are then described. An analysis of different methods in the same framework emphasizes common features and differences. This can help in choosing a more suitable method to solve a particular problem. An example of an application is finally reported.

numerical electromagnetic dosimetry   quasi-static conditions   voxel phantoms
finite difference   SPFD   current vector potential method   impedance network method

1. INTRODUCTION

1.1. What is Electromagnetic Dosimetry

Electromagnetic dosimetry is a scientific discipline aimed at studying the physical aspects of the coupling mechanisms between an electromagnetic field (EMF) and a biological object exposed to it. Coupling is the first step of a multistep interaction process which leads from exposure to biological and, possibly, health effects. The whole interaction process is intrinsically multidisciplinary, as it involves physics, biology and medicine. Nevertheless, the coupling itself is merely a physical process which involves the laws of interaction between EMFs and complex-shaped objects made with inhomogeneous, lossy materials.

Electromagnetic dosimetry applies the methods of physics to the study of this coupling mechanism, in order to determine the mathematical relationships between the intensities of the impressed EMFs and the values of the physical quantities (charges, currents, power) which the field forces induce in the tissues of the exposed body.

1.2. Basic Dosimetric Quantities

The scientific community and international radiation standard organizations generally agree in acknowledging that the physical aspects of the biological effects of EMFs are conveniently described in terms of a few physical quantities, which could be called basic dosimetric quantities. These quantities are able to properly correlate the field strengths and the intensities of the observed effects in the exposed organisms.

The standard basic dosimetric quantities are current density $\mathbf{J}$ (A/m^2) induced in the tissues of the exposed body and Specific Absorption Rate

(*SAR*) (W/kg), given by the electromagnetic power per unit mass dissipated in those tissues (Joule effect).

Current density is used for frequencies below 100 kHz, *SAR* for frequencies above 10 MHz, both of them in the 100 kHz–10 MHz frequency interval. Current density is directly proportional to the internal electric field $\mathbf{E}_i$ (V/m):

$$\mathbf{J} = \sigma \mathbf{E}_i. \tag{1}$$

The two standard basic dosimetric quantities are closely related to each other, as *SAR* is directly proportional to the square of current density:

$$SAR = \frac{\mathbf{E}_i \mathbf{J}}{\delta} = \frac{\mathbf{J}^2}{\sigma \delta} = \frac{\sigma \mathbf{E}_i^2}{\delta}. \tag{2}$$

In all these equations, σ (A/Vm) and δ (kg/m^3) are respectively electrical conductivity and mass density of the biological material.

Electromagnetic dosimetry is aimed at evaluating the basic quantities when the distribution of the impressed EMFs and the exposure conditions are known. These latter comprise (a) the shape of the exposed organism, (b) its composition, (c) the electromagnetic properties of all its parts, (d) their positions in space and (e) the geometric and electromagnetic characteristics of every object in the exposure scenario, which is the environment where exposure takes place.

To reach its intents, electromagnetic dosimetry relies on experimental, analytical or numerical techniques. Experimental dosimetry uses instrumentation and measurements to directly measure the dosimetric quantities, analytical methods are based on attempts to seek the theoretical solution of the field equations in general form, while numerical dosimetry makes use of computational techniques on digital computers to solve specific problems.

In this paper, we are particularly concerned with quasi-static dosimetry. This term refers to the application of the analytical and numerical techniques to the calculation of the induced current density distribution at low frequencies, where body dimensions are small when compared to the field wavelength.

1.3. Electromagnetic Dosimetry and Exposure Standards

Electromagnetic radiation standards, such as the International Commission on Non-Ionizing Radiation Protection (ICNIRP) Guidelines [1] or the European Directive for occupational exposure [2], usually indicate the maximum allowable values (called exposure limit values in the European Commission Directive) for the basic quantities. These values are set with reference to the thresholds of biological effects, applying proper safety margins.

Verifying compliance with exposure limit values is not a simple task, as the basic quantities can only be measured invasively. In order to simplify compliance assessment, radiation standards also specify the maximum allowable values for the intensities of the external electric and magnetic fields and for radiation power density. These values are called action values in the EC Directive [2] and should be the rms unperturbed amplitude values, i.e., field intensities measured or calculated in the exposure scenario, in the exact position occupied by the exposed subject, but in the absence of the subject itself.

In the rationale of the standards, the best available dosimetric models for standardized exposure conditions are applied (with suitable safety margins), so that compliance with action values should guarantee compliance with exposure limit values (and thus absence of adverse health effects). On the other hand, the standards allow violations of action values if it can be demonstrated, by properly using the dosimetric models in actual exposure scenarios, that exposure limit values are not violated.

2. EXPERIMENTAL DOSIMETRY

Experimental dosimetry uses instrumentation and measurements to directly measure the dosimetric quantities in exposed subjects or in artificial models called phantoms.

In-vivo measurements of induced current densities and *SAR* in humans exposed to EMFs are highly invasive and thus almost impossible for ethical reasons. Measurements on animals pose

fewer ethical problems, but their results cannot be easily extended to humans. Thus, researchers have to resort to

1. measurements of basic quantities in phantoms, as discussed further on, or
2. in-vivo measurements of some derived quantities, such as currents; induced currents (not current densities) can in fact be measured non-invasively in the following two situations.

- The total (electrically) induced current flowing to ground through the feet of an exposed body can be measured with appropriate, commercially available devices such as Holaday HI-3701 (ETS-Lingren, USA) or Narda 8854 I-MAT (Narda Safety Test Solutions GmbH, Germany). These devices consist of two horizontal plates electrically connected with a low resistance load; the subject stands on the upper plate, while the lower one is in good contact with ground, so that the load impedance is in series with the current path and the radiofrequency (RF) voltage detected across it is proportional to the current. See Hill and Walsh [3], and Gandhi, Chen and Riazi [4] for applications and results.
- The unbalanced current through a limb can be measured with "amperometric" devices based on the principle of an RF current transformer, as shown in Hagmann and Babij [5].

  All these devices usually have a usable bandwidth ranging from a few kHz to about 100 MHz.

As an alternative to in-vivo measurements, internal electric fields (hence, induced current densities, according to Equation 1) can be measured in phantoms, by using miniaturized bipolar probes. Phantoms used for these applications are simulators of biological organisms, constituted by synthetic materials designed to have dielectric properties similar to those of real biological tissues. Of course, in order to allow the probes to be inserted in them, the phantoms should be liquid or semiliquid. It could be a rather difficult task to build complex, realistic, heterogeneous liquid

or semiliquid phantoms suitable for accurate dosimetric studies.

Although rather extensively used at ELF, several difficulties (such as noise, low common mode rejection, contact impedance or electrode polarization) make this method inappropriate for accurate and reliable measurements at higher frequencies. A few of these difficulties are discussed by Geddes [6] and Gundersen and Greenebaum [7].

In the VHF band or above, phantom measurements can be performed with fewer difficulties using integrated probe-and-diode detector devices. Thanks to the square low of detection, these devices have a DC output voltage which is directly proportional to *SAR*. For really intrinsic *SAR* measurements, thermometric rather than semiconductor detectors can be used, as in implantable miniaturized thermocouple or thermistor probes. With these devices, *SAR* is evaluated from the initial rate of increase of the local temperature *T* due to the RF power absorption during exposure:

$$SAR = c\frac{\Delta T}{\Delta t}, \tag{3}$$

where c, in J/kg $^{\circ}$C, is the specific heat of the phantom material. A similar principle, but based on a visual rather than an electrical signal acquisition (thus requiring a transparent phantom), is behind the use of infra-red thermocameras and thermocromic liquid crystal plates.

In conclusion, experimental dosimetry has to face several problems. Although some of them could be partially overcome with further research, it seems unlikely that these techniques will play a decisive role in future applications, apart from being used as a check for numerical methods.

3. THEORETICAL DOSIMETRY: THE QUASI-STATIC APPROACH

Low-frequency applications of theoretical (i.e., analytical and numerical) dosimetry take advantage of the quasi-static approximation (QSA), which has been extensively applied up to a few tens of megahertz. According to this approach,

the analysis of the interactions between biological systems and low-frequency electric or magnetic fields is greatly simplified if the following three conditions are satisfied [8].

1. The dimensions of the involved objects and their mutual distances should be small when compared to the free-space wavelength. This condition ensures that propagation effects will be negligible. The practical consequence is that electric and magnetic fields generated by given distributions of charges and currents can be calculated using the methods of electrostatics and magnetostatics.
2. The size of the exposed subject should be comparable to, or smaller than, the magnetic skin depth in the biological materials. See Table 1 for the values of the magnetic skin depth at some frequencies, for a few representative

human body tissues. This condition guarantees that the effects of the magnetic fields produced by currents induced in the tissues will be small and thus the applied magnetic field will be essentially unperturbed by the exposed body.

3. In the exposed subject, conduction currents should prevail over displacement currents. As a consequence, charge movements will follow "instantaneously" the oscillations of the fields (charges move and rearrange in phase with the internal electric field), the body can be considered equipotential and the calculation of the electric fields outside and inside it can be separated into two distinct problems, as it will be shown further on. In order to evaluate this condition, the values of loss tangent are depicted in Figure 1 as a function of frequency for a few representative human body tissues.

TABLE 1. Magnetic Skin Depths at Selected Frequencies Between 1 kHz and 10 MHz, for a Few Representative Human Body Tissues

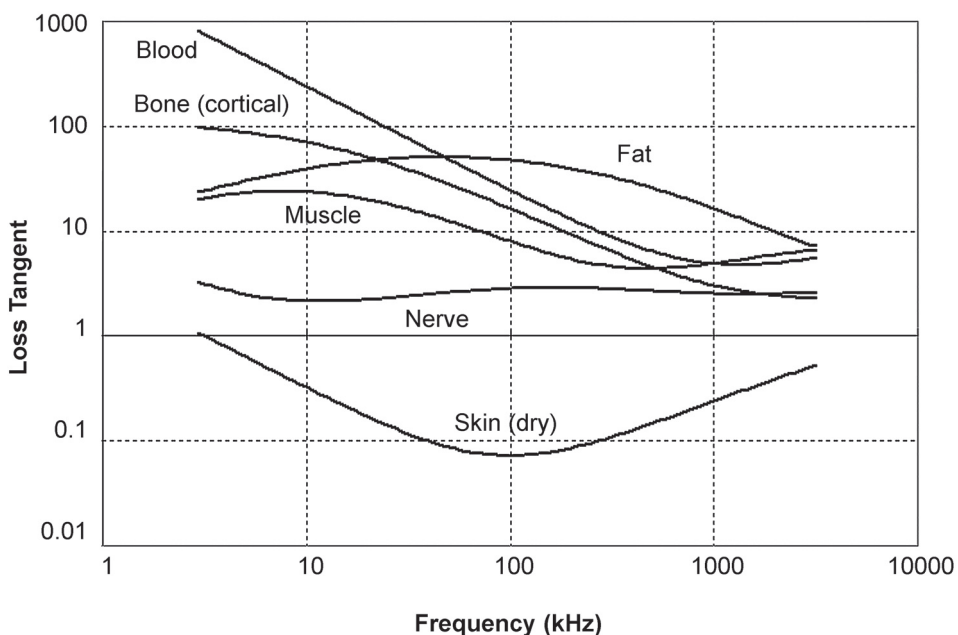| Frequency	Magnetic Skin Depth (m)					
	Blood	Muscle	Fat	Bone (cortical)	Nerve	Skin (dry)
1 kHz	19	29.2	110	113	100	1314
10 kHz	6.03	8.81	33.0	35.5	30.6	887
100 kHz	1.94	2.82	10.3	11.4	6.66	394
1 MHz	0.615	0.785	3.28	3.79	1.69	12.7
10 MHz	0.163	0.219	1.06	0.969	0.407	0.561

Figure 1. Dielectric loss tangent as a function of frequency between 1 kHz and 10 MHz, for a few representative human body tissues.

Loss tangent is in fact defined as the ratio of the conduction current over the displacement current:

$$\text{Loss tangent} = \frac{\sigma}{2\pi f \varepsilon \varepsilon_0}, \qquad (4)$$

where σ and ε are the electrical conductivity and the relative permittivity of the tissue and ε_0 is the absolute permittivity of the free space.

Thus, thanks to the QSA, the electric and the magnetic field problems get decoupled and can be solved separately. Furthermore, each of these problems can be broken into two separate steps.

1. In the first step (the external problem), the solution of the static field equations (those obtained by completely removing the time derivatives from Maxwell equations) leads to a sufficiently accurate evaluation of the electric and magnetic fields external to the exposed subject and of the surface-charge density on its boundary. At this stage, the subject is regarded as a homogeneous, equipotential and perfectly conductive body.

2. In order to determine the physical quantities inside the body (second step, the internal problem), the time derivatives are reintroduced into the equations, and internal electric fields and current densities are computed on the basis of the results of the previous step.

With the QSA, we are left with the need to ascertain how low the frequency should be for this approach to give sufficiently accurate results. The answer depends, of course, on the degree of accuracy that we are seeking. Strictly speaking, the three QSA conditions hold at most up to a few hundred kilohertz, but in the literature this approach is often assumed valid also for higher frequencies, up to a few tens of megahertz.

3.1. Coupling to the Electric Field

To solve the external problem, the electric potential of the exposed biological object (considered a homogeneous perfect conductor) is regarded as constant, hence the internal electric field is null. The impressed electric field is perturbed by the object, so that the field lines are perpendicular to its outer surface. The perturbation depends on the shape of the object, but not on its size or conductivity. The Laplace equation is solved and the surface-charge and displacement current densities are computed at the body boundary.

Coming to the internal problem, the assumption of a perfect conductor is removed; the previously-calculated surface charge and current densities serve as boundary conditions for the calculation of the internal electric potential distribution; from the potential differences the internal electric field, hence the volume current density, distributions are computed.

3.2. Coupling to the Magnetic Field

Because biological materials do not possess ferromagnetic properties, they do not directly distort the impressed magnetic field. Even the scattered fields produced by induced currents are negligible. The solution of the external problem is thus trivial: the total field is equal to the impressed field and can be calculated by means of standard techniques, like those based on the Biot-Savart law or on the magnetic potential approach.

For what concerns the internal problem, a time-changing magnetic field produces an electric field whose lines form closed loops and have shapes determined by the boundary of the medium. If the medium is a biological object with nonzero conductivity, an induced (eddy) current will flow. Its distribution can be calculated with methods based on the application of the Faraday law.

4. ANALYTICAL DOSIMETRY

Analytical dosimetry is aimed at finding a solution to the set of Maxwell equations which describes the coupling of the EMF with the exposed body, taking source characteristics and environment properties into account, with the help of the QSA and with reference to some particularly simplified geometries, like the sphere, the cylinder, the spheroid and the ellipsoid, in free space or over an infinite, perfectly conducting ground plane.

Spherical and cylindrical boundary objects are studied in McLeod, Pilla and Sampsel [9] and in Polk [10]. Objects, considered good conductors,

are exposed to magnetic fields from ELF up to 3 MHz. In the simpler case (field parallel to the axis), the solution for the cylinder is reached through the use of Bessel equations and hence Bessel functions of the first kind.

Durney, Johnson and Massoudi [11] developed an important application of the perturbation theory (Stevenson's method). In this application, electric and magnetic fields are expanded in a power series of the free-space propagation constant k_0; series expressions are substituted in field and boundary-condition equations and the coefficients of corresponding powers of k_0 in the resulting system of equations are equated. At sufficiently low frequencies, the electric field inside the exposed object can be approximated by the zeroth- and first-order terms in k_0, higher order terms being negligible. Expressions for these lower order terms are then obtained by appropriate equations, which are easier to solve than the original Maxwell ones, because they just require the solution of the Laplace equation in proper co-ordinate systems. This method has been applied to compute the electromagnetic absorption in prolate spheroidal [11, 12] and ellipsoidal [13, 14] models of a man; according to the authors, for a man-size object this approach is valid up to 30 MHz.

In general, analytical methods suffer from a few major intrinsic limitations, which severely penalize their applications to realistic problems. They cannot easily accommodate complex environments, particular postures (outstretched arms, for instance), different grounding patterns (no, one or two legs grounded) or internal body structure.

Nevertheless, analytical models are valuable because they often provide an insight into the qualitative nature of the coupling mechanisms. As for experimental dosimetry, analytical results are also useful as a check for numerical techniques.

5. NUMERICAL DOSIMETRY

Numerical dosimetry uses numerical methods to solve field equations by means of digital computers and computational techniques. It is going to become the preferred electromagnetic dosimetry approach, as it benefits the continuously increasing performance (speed and memory storage, in particular) and the decreasing costs of information technology products. Applications to more and more complex problems should be expected, involving multiple sources, realistic environments and accurate modeling of exposed subjects, as needed to properly analyze occupational exposure situations. As a counterpart, one has to abandon the "general" point of view typical of the analytical approach and concentrate on specific problems.

Quasi-static applications of numerical dosimetry are conveniently described following an approach which involves the following steps.

1. The impressed (unperturbed) electric and/or magnetic fields are calculated.
2. The exposed subject (or part of it) is segmented, i.e., subdivided into small homogeneous elements.
3. Values for the dielectric properties are assigned to each element.
4. A set of differential or integral equations modeling the problem being considered is developed.
5. A system of algebraic equations is derived from the preceding steps.
6. This system is finally solved by means of a suitable numerical algorithm.

5.1. Calculation of Impressed Field

Reference levels (or action values) specified by international RF safety standards (such as the ICNIRP Guidelines [1] or the EC Directive [2]) refer to the intensities of the impressed fields, so calculation of the impressed electric and/or magnetic fields should be the first step. Impressed fields are the electric and magnetic fields which are present on the site of the exposed subject, when the exposed subject is absent. They are generated by sources and are possibly perturbed by objects in the exposure scenario.

5.1.1. Impressed electric field

Calculation of the impressed electric field in quasi-static conditions is usually based on the numerical solution of the Laplace equation for the electric potential, whose value should be given on the

sources and on other objects present in the exposure scenario. Adopting a finite-difference scheme of the solution, an algebraic system of equations can be obtained; its solution is usually achieved through the successive over-relaxation technique [15].

Alternatively, the surface-charge integral equation approach can be used. This approach leads to an equation that links the electric potential at any point to the charge density on the boundary surfaces of the sources and other objects. The integral equation can be solved for the charge density following a standard algorithm based on the method of moments (MOM), assuming the potential is known on every object in the exposure scenario. Once the charge density has been calculated, the electric potential (hence the electric field) can be computed in every point.

5.1.2. Impressed magnetic field

Calculation of the impressed magnetic field generated by a given current distribution in quasi-static conditions is usually based on the numerical integration of the Biot-Savart equation in a differential form. Alternatively, one could resort to the use of the magnetic vector potential approach, i.e., calculate the vector potential by integrating the current distribution and then calculate the magnetic flux density by numerically taking the curl of the vector potential.

5.2. Body Segmentation

Segmentation, the second step, is the process of building a discrete mathematical model of the exposed subject, subdividing it into segments, i.e., small homogeneous elements with regular geometry (usually square pixels in two-dimensional problems or cubic voxels in three-dimensional problems). Of course, the lower the segment size, the higher the accuracy of the results. On the other hand, higher resolutions demand higher computational resources, as all numerical methods have storage and time requirements proportional to the number of segments.

While older works relied on atlases of anatomical cross-sections, more recent ones make mostly use of the Magnetic Resonance Imaging (MRI) technique as a source of anatomic data that have to be (semi)automatically processed in order to recognize different tissue types [16, 17]. Norman (the NORmalized MAN) [17, 18] is probably the most representative example of this approach. Norman consists of a three-dimensional parallelepiped-shaped regular array of nearly 36 million homogeneous voxels, modeling a standardized human body (1.76 m height, 73 kg mass) and some surrounding space (8.3 million cells are in the body, the remaining in the surrounding space). Each cell has a roughly cubic shape (~2 mm size) and is labeled with a tag denoting its tissue type, chosen from a palette of 37 different tissues. This process is automatically achieved interpreting the gray scale data of MRI images.

An even higher-resolution digital model of a man (voxel size down to 1 mm) has been developed at the Radio Frequency Radiation Branch of the Brooks U.S. Air Force Base Research Laboratory [19], using the Library of Medicine Visible Human Project (VHP) dataset [20].

5.3. Advanced Numerical Models of the Human Body

The development of numerical models of the human body plays an important role in exposure assessment. Available digital body models usually represent the human body in the standing position and cannot be directly used for dosimetric evaluations in different postures, as required by occupational exposure studies.

The development of a flexible human model can be carried out using different approaches, depending on the use for which the model is designed. For virtual surgery, for example, it is important to represent every part of the body with the finest possible details. In the case of numerical dosimetry, the body model has to be put in different postures and the continuity of tissues must be ensured, but a hyper-realistic articulation model is not compulsory. It would be more interesting to use the same approximated articulation approach on different body models, rather than to have a hyper-realistic model which fits a particular phantom only.

At IFAC-CNR (Institute for Applied Physics "Nello Carrara" of the Italian National Research Council), an articulation algorithm is under development to be used in conjunction with finite-

difference numerical techniques. This approach is aimed at achieving a compromise between the realism of the articulation and the applicability of the same approach to different joints and different body models.

In general, the articulation process deforms the voxels close to the joint, so that the articulated body model has to be re-sampled over a regular grid before it can be used as a base for finite-difference calculation. Re-sampling can be a critical step, particularly to ensure mass conservation before and after the articulation process. The algorithm under development tries to take into account the need of having cubic voxels at the end of the process. This is done by isolating the joint district and building an elastic model which separates voxels that undergo rigid translations and rotations (bones, for example) from voxels that go through elastic deformations (fleshy parts).

The imaginary box that contains the joint district plays a key role. A set of control points placed over the box regulates the elastic deformations of fleshy parts. Portions of the body out of the joint district undergo only translations and rotations, but not deformations.

Figure 2 shows the results of the articulation of the knee in the sagittal plane with an articulation angle of 90°. The knee model at rest used in the example was extracted from the Brooks voxel phantom [19].
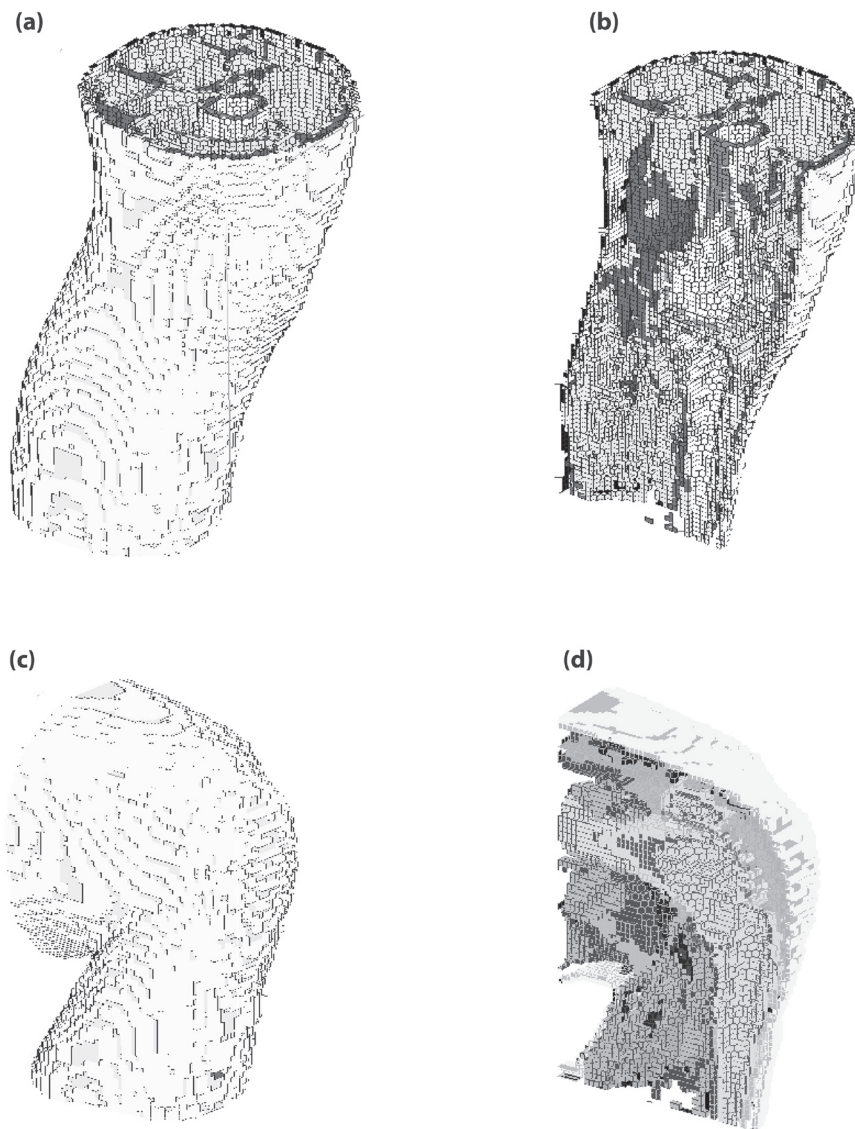

Figure 2. Example of articulation of the knee. Rest position: (a) external view, (b) sagittal cross section. Articulation angle of 90° in the sagittal plane: (c) external view; (d) sagittal cross section.

5.4. Dielectric Properties of Body Tissues

Once the exposed subject has been segmented, values for the dielectric properties (i.e., the conductivity σ and the relative permittivity ε) have to be assigned to each segment, taking frequency into account. This is usually accomplished through a preliminary assessment of the type of tissue each segment is composed of and the subsequent application of the Gabriel model.

Gabriel and colleagues, in a thorough work, have in fact developed a parametric model able to represent the dielectric properties of biological tissue in the frequency range from 10 Hz to 100 GHz and have determined the values of the model parameters for 45 different human tissues, by fitting in the model both the literature-available experimental data and their own original measurements [21, 22]. Internet applications have also been developed and are currently available [23, 24]; they adopt Gabriel's model to allow on-line calculation and downloading the values of relative permittivity, electrical conductivity and a few derived parameters of about 50 different human body tissues in the frequency range from 10 Hz to 100 GHz.

An alternative approach which deserves a citation is aimed at directly determining the dielectric properties of each voxel, without passing through the tissue recognition process [25]. This approach is based on the evaluation of the tissue water content by means of an automatic processing of the MRI images. For this reason, its applicability is limited to frequencies approximately above 100 MHz.

5.5. Numerical Modeling

Numerical modeling is the next step. A set of differential or integral equations with proper boundary conditions, suitable for describing the problem being considered, should be developed. These equations should then be put into a discrete form, i.e., should be adapted to the segmented model of the exposed subject. This way, a system of linear algebraic equations is derived, to be numerically solved using standard computational algorithms.

Several methods have been proposed, with specific advantages and limitations [26]. Among the most popular ones, at least in the academic and research world, we can cite

- the MOM [27], particularly useful for solving low-resolution problems modeled with integral equations, like in Chen, Chuang and Lin [28];
- the finite-difference family of methods [29], which also comprises the impedance network method [30], well-suited for high-resolution, quasi-static, two- or three-dimensional problems expressed by means of a system of linear differential equations, like in Dawson, Caputa and Stuchly [31], Dimbylow [32] and DeFord and Gandhi [33];
- the finite difference time domain (FDTD) method [34, 35], today the preferred choice for high frequency problems.

It can be useful to recall and compare a few computational properties of these methods [33, 35]. In an N cell problem, the MOM requires computer storage proportional to N^2 and computation time proportional to N^3. This situation becomes prohibitive when dealing with high resolution heterogeneous models. Finite-difference-like methods (including FDTD and impedance network methods), on the contrary, have storage and time requirements proportional to N. On the other hand, the number of cells N is substantially larger in the finite-difference, FDTD and impedance network methods than in the MOM, because of the overhead of free-space cells surrounding the body, necessary to guarantee proper boundary conditions.

As already mentioned, thanks to the QSA, numerical modeling can be split into four independent problems, separating external from internal problems and electric from magnetic field problems.

5.6. External Problem

According to the QSA, the external electric and magnetic fields in the presence of the exposed body are calculated using the methods of electrostatics and magnetostatics, which also lead to a sufficiently accurate evaluation of the

surface-charge density on the body boundary. The quantities calculated at this stage will then serve as the driving terms and boundary conditions for the calculation of the induced current density.

5.6.1. External problem for the electric field

Approaches used to solve the external problem for the electric field are quite similar to those seen for the calculation of the impressed electric field (section 5.1.1.), but with two fundamental differences:

- the exposed subject should be present in the exposure scenario; it is regarded as homogeneous, equipotential and perfectly conductive, hence the internal electric field is null;
- we are not interested in calculating the electric field itself; we are mainly interested in calculating the surface-charge density on the external boundary of the exposed subject.

As for the solution of the impressed field problem, two main approaches are used. The first one is based on the finite-difference solution of the Laplace equation for the electric potential outside the body [36]; the surface-charge density on the body boundary is then computed from the normal gradient of the potential. The second one is an application of the MOM to solve the surface-charge density integral equation [28]:

$$\varphi_b = \varphi_s(Q) + \varphi_i(Q),$$
$$\varphi_s(Q) = \frac{1}{4\pi\varepsilon_0} \int_\Sigma \frac{\eta(P)}{|Q - P|} d\Sigma. \qquad (5)$$

Here, Q is a generic point in the body and P is a point on its boundary surface Σ. The body potential φ_b (unknown, but assumed spatially constant) is expressed as the sum of the potential φ_s maintained by the induced unknown surface charge η on the body boundary Σ and the potential φ_i (assumed known) maintained by the impressed electric field sources. A second equation involving the two unknown η and φ_b is of course needed, and is obtained on the basis of the Ohm law:

$$\varphi_b = j\omega Z_{eq} \int_\Sigma \eta(P) d\Sigma, \qquad (6)$$

where Z_{eq} is the total equivalent body grounding impedance, which has to be estimated.

5.6.2. External problem for the magnetic field

As already noted (section 3.2.), the solution of the external problem for the magnetic field is trivial, as it is reduced to the calculation of the impressed magnetic field, an aspect already treated in section 5.1.2.

5.7. Internal Problem

According to the principles of the QSA, in order to determine the basic physical quantities induced inside the body (current density and *SAR*), the time derivatives are reintroduced into the equations (when required) and the internal electric field and current density values are computed, using the results of the solution of the external problem as boundary conditions.

5.7.1. Current density induced by electric field

The most common approach relies on the application of the Laplace equation for the internal electric potential [36], using the previously-calculated surface-charge density as the boundary condition. This equation is in fact easily obtained combining the electrostatic representation of the internal electric field $\mathbf{E}_i$ as a gradient of a scalar function φ, with the Ampere-Maxwell curl equation for the scattered magnetic field $\mathbf{H}_S$ (generated by the induced currents):

$$\begin{cases} \mathbf{E}_i = -\nabla\varphi \\ \nabla \times \mathbf{H}_S = \mathbf{J} \\ \mathbf{J} = \sigma\mathbf{E}_i \end{cases} \Rightarrow \nabla \cdot (\sigma\nabla\varphi) = 0. \qquad (7)$$

From potential differences the internal electric field and, hence, volume current density values, are then computed.

5.7.2. Current density induced by magnetic field

The most popular methods for solving three-dimensional problems are probably the impedance

network method and the scalar potential finite difference (SPFD) method (see sections 5.8.1. and 5.8.3.). They are compared from the point of view of accuracy and speed in Dimbylow [37], where the calculation of the current density distribution in the Norman model for uniform, quasi-static magnetic field exposure is presented. Quasi-static conditions are assumed valid up to 10 MHz. As noted by the author, the impedance network method is basically a vector method, whereas the SPFD method is innately scalar (i.e., it leads to a scalar equation even in the most complicated three-dimensional geometry). The former requires 27 million words to store the three components of the loop current values in Norman, compared to the 9 million words required to store the potential values in the SPFD method. Furthermore, the computational molecule for the SPFD method is more compact and requires fewer arithmetic operations, so that the computational time per iteration needed by the impedance network method is nearly twice that required by the scalar potential method.

5.8. Popular Numerical Methods

Among the numerical methods most widely used for low-frequency, quasi-static electromagnetic dosimetry problems, three deserve to be briefly described with a few details: the impedance network method, the current vector potential method and the SPFD method.

5.8.1. The impedance network method

In the three-dimensional impedance network method [33, 37], each cubic element (cell) generated with the segmentation process is further differentiated into a three-dimensional network of impedances. Every cell is represented by three impedances located on three of its edges, sharing a common vertex. The value of each edge impedance is determined averaging the complex conductivity values of its four neighboring cells. At last, the whole exposed body is represented by a linear circuit and the circuit theory is applied to compute the currents in the impedances. This approach leads to a system of coupled Kirchhoff current law equations, to be solved using an iterative process.

In magnetic-field-only exposure problems, the time-varying impressed magnetic flux density induces voltage in each closed loop formed by four connected impedances in one plane, according to the Faraday law. On the basis of the Kirchhoff current law, the solution for the impedance currents in this case is achieved by equating the induced voltage to the sum of the edge currents times impedances around each loop.

If an impressed electric field is also present, then the charge density on the subject boundary surface must be determined in advance and then used to calculate the current injected in the impedances at boundary cells, by means of the continuity equation for the electric charge.

5.8.2. The current vector potential method

The basic equation of the current vector potential method [38] is obtained by combining the Ampere curl equation for the scattered magnetic field $\mathbf{H}_S$ (generated by the induced currents) with the Faraday-Maxwell curl equation relating the induced electric field $\mathbf{E}_i$ to the time-derivative of the impressed magnetic flux density $\mathbf{B}_0$:

$$\left.\begin{cases} \nabla \times \mathbf{H}_S = \mathbf{J} \\ \mathbf{J} = \sigma\mathbf{E}_i \\ \nabla \times \mathbf{E}_i = -\dfrac{\partial \mathbf{B}_0}{\partial t} \end{cases}\right\} \Rightarrow \nabla \times \left(\frac{1}{\sigma} \nabla \times \mathbf{H}_S \right) = -\frac{\partial \mathbf{B}_0}{\partial t}. \tag{8}$$

Applications of this technique are usually limited to two-dimensional, magnetic-field-only problems, because in this case it leads, as one can easily find, to a scalar differential equation, which can be solved by means of a standard finite-difference algorithm. However, the method is not well suited for electric field exposure dosimetric evaluations, because the surface-charge density boundary conditions can not be easily accommodated.

5.8.3. The SPFD method

The SPFD method [37, 38] is particularly suited for solving three-dimensional problems, because it always leads to a scalar equation. In the next sections it is shown how the scalar equation can be obtained starting from Maxwell laws.

The SPFD equation

The SPFD formulation can be obtained on the basis of both the Faraday-Maxwell curl equation for the electric field and the Ampere-Maxwell curl equation for the magnetic field. In the Faraday-Maxwell equation, the magnetic flux density is expressed as the curl of an impressed magnetic potential:

$$\nabla \times \mathbf{E} = -j\omega \mathbf{B} = -j\omega \nabla \times \mathbf{A}. \tag{9}$$

Thanks to this, electric scalar potential φ is also introduced:

$$\nabla \times (\mathbf{E} + j\omega \mathbf{A}) = 0 \quad \Rightarrow \quad \mathbf{E} + j\omega \mathbf{A} = -\nabla \varphi$$
$$\Rightarrow \quad \mathbf{E} = -j\omega \mathbf{A} - \nabla \varphi. \tag{10}$$

The last expression is now put into the Ampere-Maxwell curl equation for the magnetic field:

$$\nabla \times \mathbf{H} = (\sigma + j\omega\varepsilon)\mathbf{E} = (\sigma + j\omega\varepsilon)(-\nabla \varphi - j\omega\mathbf{A}). \tag{11}$$

Applying the divergence operator to the first and the last terms of Equation 11, one obtains

$$\nabla \cdot [(\sigma + j\omega\varepsilon)(-\nabla \varphi - j\omega\mathbf{A})] = 0. \tag{12}$$

This is the standard SPFD formulation. It is valid in general, but can be easily solved in quasi-static conditions only. In that case, the vector potential $\mathbf{A}$ can be assumed known (as generated by the external magnetic field sources) and the scalar potential φ becomes a unique unknown. Furthermore, in quasi-static conditions $\sigma \gg \omega\varepsilon$ and the SPFD equation becomes

$$\nabla \cdot [\sigma(-\nabla \varphi - j\omega\mathbf{A}_{\text{sources}})] = 0. \tag{13}$$

Once this equation has been solved and the scalar potential calculated, the internal electric field $\mathbf{E}_i$ and the current density $\mathbf{J}$ can be calculated with the following expressions:

$$\mathbf{E}_i = -\nabla \varphi - j\omega \mathbf{A}_{\text{sources}} \tag{14}$$
$$\Rightarrow \quad \mathbf{J} = \sigma \mathbf{E}_i = \sigma(-\nabla \varphi - j\omega \mathbf{A}_{\text{sources}}).$$

Boundary conditions

The SPFD equation must be solved inside the body volume; thanks to the QSA, the forcing terms accounting for external electric and magnetic field sources can be considered separately. While the vector potential $\mathbf{A}_{\text{sources}}$ accounts for the magnetic field, if an external electric field is also present, the condition

$$\sigma \mathbf{E}_i \cdot \hat{n} = j\omega\eta \tag{15}$$

must be imposed on the body surface. $\mathbf{E}_i$ is the electric field inside the body and η is the surface charge density, calculated previously by solving the external Laplace problem for the electric field; $\hat{n}$ is the outward normal unit vector on the body surface. Clearly, Equation 15 is just the current continuity (or charge conservation) expression on the surface: no supplementary boundary conditions are needed on that surface in order to solve the problem, as the SPFD equation is itself a particular formulation of the current continuity condition.

The discretization of the scalar equation

In order to build a segmented or discrete form of the SPFD equation, one has to start from the integral form of Equation 13, which in turn can be easily obtained by applying the divergence theorem.

The following expression, valid in two dimensions, adopts the Dimbylow discretization scheme [37] and links the unknown scalar potential φ_0 in a cell vertex to the potential values taken in the four neighboring vertexes. The known coefficients are the averaged conductivities between cells σ_{mi} and the proper component $\mathbf{A}_{\text{mi}}$ of the source-generated vector potential:

$$\varphi_0 = \left(\frac{1}{\displaystyle\sum_{i=1}^{4} \sigma_{\text{mi}}}\right) \cdot \sum_{i=1}^{4} \left\{ \sigma_{\text{mi}} \left[\varphi_i - (-1)^i j\omega l_c A_{\text{mi}} \right] \right\} \tag{16}$$

The three-dimensional discretization scheme is a straightforward extension of the two-dimensional case. For every "central" vertex (index 0), six neighboring vertexes should be considered instead of four. The segmented SPFD expression is then the following:

$$\varphi_0 = \left(\frac{1}{\displaystyle\sum_{i=1}^{6} \sigma_{\text{mi}}}\right) \cdot \sum_{i=1}^{6} \left\{ \sigma_{\text{mi}} \left[\varphi_i - (-1)^i j\omega l_c A_{\text{mi}} \right] \right\} \tag{17}$$

Border of the calculation domain

When a finite-difference numerical method is used, the solution of the problem on the border of the considered domain requires particular attention. In many numerical dosimetry problems, the body is isolated from ground, as if it were immersed inside an imaginary box full of nonconductive material, which has to be more or less large according to the computational requirements.

In the present case, thanks to the particular SPFD discretization scheme, the volume that should be taken into account coincides with body volume only. This is a consequence of the fact that the scalar potential values in conductive regions (border included) are not influenced by values in nonconductive ones. In fact, the terms that link the values of the scalar potential between neighboring vertexes in the SPFD equation in discrete form, are the average conductivities taken half-way, and the average conductivities that link cells vertexes on the border of the conductive region with outer vertexes are null.

6. EXAMPLE OF APPLICATIONS

Figure 3 shows a view of the median sagittal section of the current density distribution induced in the head of the Brooks model [19] exposed to a uniform magnetic flux density of 1 mT at 100 Hz. To solve the problem in three dimensions, the SPFD method was used. The finite difference problem was solved using the successive over-relaxation technique. Even if faster methods do indeed exist, successive over-relaxation has the great advantage of being easier to code even in three-dimensional cases [39].

7. CONCLUSIONS

While analytical and experimental techniques seem to face their limits, numerical methods currently play a key role in electromagnetic dosimetry and have a promising future. However, a lot of research is still needed to produce accurate, articulated, very high resolution digital models of the human
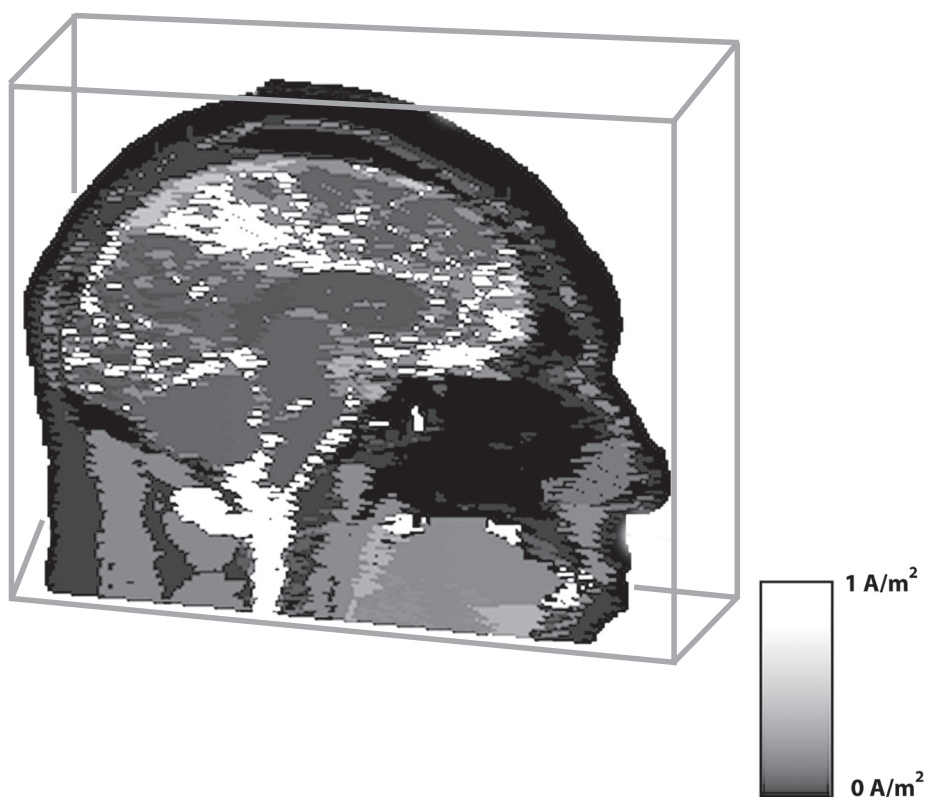

Figure 3. Example of results: current density distribution inside a head exposed to a uniform magnetic flux density of 1 mT at 100 Hz, calculated with the SPFD method. *Notes.* SPFD—scalar potential finite difference.

body and to achieve a better knowledge of the dielectric properties of its tissues, particularly at lower frequencies.

Among the available numerical methods for quasi-static applications, the SPFD approach appears to be the most suitable to cope with articulated phantoms in complex three-dimensional problems, like those met in occupational environment exposure.

REFERENCES

1. International Commission on Non-Ionizing Radiation Protection. Guidelines for limiting exposure to time-varying electric, magnetic and electromagnetic fields (up to 300 GHz). Health Phys. 1998;74(4):494–522.

2. Directive 2004/40/EC of the European Parliament and of the Council of 29 April 2004 on the minimum health and safety requirements regarding the exposure of workers to the risks arising from physical agents (electromagnetic fields) (eighteenth individual Directive within the meaning of Article 16(1) of Directive 89/391/EEC). Official Journal of the European Union L 184, May 24, 2004. p. 1–9.

3. Hill DA, Walsh JA. Radio-frequency current through the feet of a grounded human. IEEE Trans Electr Compat. 1985;EMC-27(1): 18–23.

4. Gandhi OP, Chen JY, Riazi A. Currents induced in a human being for plane–wave exposure conditions 0–50 MHz and for RF sealers. IEEE Trans Biomed Eng. 1986;BME-33(8):757–68.

5. Hagmann MJ, Babij TM. Noninvasive measurement of current in the human body for electromagnetic dosimetry. IEEE Trans Biomed Eng. 1993;BME-40(5):418–23.

6. Geddes LA. Interface design for bioelectrode systems. IEEE Spectr. 1972;9(10):41–8.

7. Gundersen R, Greenebaum B. Low-voltage ELF electric field measurements in ionic media. Bioelectromagnetics. 1985;6:157–68.

8. Kaune WT, Guttman JL, Kavet R. Comparison of coupling of humans to electric and magnetic fields with frequencies between 100 Hz and 100 kHz. Bioelectromagnetics. 1997;18:67–76.

9. McLeod BR, Pilla AA, Sampsel MW. Electromagnetic fields induced by Helmholtz aiding coils inside saline-filled boundaries. Bioelectromagnetics. 1983;4:357–70.

10. Polk C. Electric fields and surface charges induced by ELF magnetic fields. Bioelectromagnetics. 1990;11:189–201.

11. Durney CH, Johnson CC, Massoudi H. Long-wavelength analysis of plane wave irradiation of a prolate spheroid model of man. IEEE Trans MTT. 1975;MTT-23(2):246–53.

12. Johnson CC, Durney CH, Massoudi H. Long-wavelength electromagnetic power absorption in prolate spheroidal models of man and animals. IEEE Trans MTT. 1975;MTT-23(9):739–48.

13. Massoudi H, Durney CH, Johnson CC. Long-wavelength analysis of plane wave irradiation of an ellipsoidal model of man. IEEE Trans MTT. 1977;MTT-25(1):41–6.

14. Massoudi H, Durney CH, Johnson CC. Long-wavelength electromagnetic power absorption in ellipsoidal models of man and animals IEEE Trans MTT. 1977:MTT-25(1):47–52.

15. Binns KJ, Lawrenson PJ. Analysis and computation of electric and magnetic field problems. 2nd ed. Oxford, UK: Pergamon Press; 1973.

16. Cheng J, Stuchly MA, DeWagter C, Martens L. Magnetic field induced currents in a human head from use of portable appliances. Phys Med Biol. 1995;40: 495–510.

17. Dimbylow PJ. FDTD calculations of the whole-body averaged SAR in an anatomically realistic voxel model of the human body from 1 MHz to 1 GHz. Phys Med Biol. 1997;42:479–90.

18. Dimbylow PJ. The development of realistic voxel phantoms for electromagnetic field dosimetry. In: Proceedings of the International Workshop on Voxel Phantom Development. Chilton, UK: National Radiological Protection Board; 1996. p. 1–7.

19. U.S. Air Force Research Laboratory. EMF dosimetry research. Brooks Air Force Base, TX, USA. Retrieved April 20, 2006, from: http://www.brooks.af.mil/AFRL/HED/hedr/dosimetry.html

20. U.S. National Library of Medicine. The Visible Human Project®. Retrieved April 20, 2006, from: http://www.nlm.nih.gov/research/visible/visible_human.html

21. Gabriel C, Gabriel S, Corthout E (part I only), Lau RW (parts II and III only). The dielectric properties of biological tissues (part I, II and III). Phys Med Biol. 1996;41:2231–93.

22. Gabriel C, Gabriel S. Compilation of the dielectric properties of body tissues at RF and microwave frequencies. Retrieved April 20, 2006, from: http://www.brooks.af.mil/AFRL/HED/hedr/reports/dielectric/home.html

23. U.S. Federal Communications Commission. Tissue dielectric properties. Retrieved April 20, 2006, from: http://www.fcc.gov/cgi-bin/dielec.sh

24. Institute for Applied Physics "Nello Carrara" (IFAC) of the Italian National Research Council (CNR). Dielectric properties of body tissues. Retrieved April 20, 2006, from: http://niremf.ifac.cnr.it/tissprop/

25. Farace P, Pontalti R, Cristoforetti L, Antolini R, Scarpa M. An automated method for mapping human tissue permittivities by MRI in hyperthermia treatment planning. Phys Med Biol. 1997;42:2159–74.

26. Hart FX. Numerical and analytical methods to determine the current density distributions produced in human and rat models by electric and magnetic fields. Bioelectromagnetics. 1992;Suppl 1:27–42.

27. Harrington RF. Field computation by moment methods. New York, NY, USA: Macmillan; 1968.

28. Chen KM, Chuang HR, Lin CJ. Quantification of interaction between ELF-LF electric fields and human bodies. IEEE Trans Biomed Eng. 1986;BME-33(8):746–56.

29. Booton Jr RC. Computational methods for electromagnetics and microwaves. New York, NY, USA: Wiley; 1992.

30. Gandhi OP, DeFord JF, Kanai H. Impedance method for calculation of power deposition patterns in magnetically induced hyperthermia. IEEE Trans Biomed Eng. 1984;BME-31(10):644–51.

31. Dawson TW, Caputa K, Stuchly MA. Numerical evaluation of 60 Hz magnetic induction in the human body in complex occupational environments. Phys Med Biol. 1999;44:1025–40.

32. Dimbylow PJ. Current densities in a 2 mm resolution anatomically realistic model of the body induced by low frequency electric fields. Phys Med Biol. 2000:45:1013–22.

33. DeFord JF, Gandhi OP. An impedance method to calculate currents induced in biological bodies exposed to quasi-static electromagnetic fields. IEEE Trans Electr Compat. 1985;EMC-27(3):168–73.

34. Kunz KS, Luebbers RJ. The finite difference time domain method for electromagnetics. Boca Raton, FL, USA: CRC Press; 1993.

35. Sullivan DM, Borup DT, Gandhi OP. Use of the finite-difference time-domain method in calculating EM absorption in human tissues. IEEE Trans Biomed Eng. 1987: BME-34(2):148–58.

36. Dimbylow PJ. The calculation of induced currents and absorbed power in a realistic, heterogeneous model of the lower leg for applied electric fields from 60 Hz to 30 MHz. Phys Med Biol. 1988;33:1453–68.

37. Dimbylow PJ. Induced current densities from low-frequency magnetic fields in a 2 mm resolution, anatomically realistic model of the body. Phys Med Biol. 1998;43: 221–30.

38. Davey KR, Cheng CH, Epstein CM. Prediction of magnetically induced electric fields in biological tissue. IEEE Trans Biomed Eng. 1991;BME-38(5):418–22.

39. Press WH, Teukolsky SA, Vetterling WT, Flannery BF. Numerical recipes in C: the art of scientific computing. 2nd ed. Cambridge, UK: Cambridge University Press; 1992.